Geotechnical Aspects of Underground Construction in Soft Ground – Yoo, Park, Kim & Ban (Eds)
© 2014 Korean Geotechnical Society, Seoul, Korea, ISBN 978-1-138-02700-8

Reinforcing mechanism of anchor type retaining wall – model test and numerical analysis

T. Nakai
Geo-Research Institute, Nagoya, Japan

H.M. Shahin
Nagoya Institute of Technology, Nagoya, Japan

K. Okuda
Penta-Ocean Construction, Miyagi, Japan

M. Kato
Central Japan Railway, Gifu, Japan

ABSTRACT: To investigate fundamental mechanism of the ground behavior in braced excavation using ground anchors, two-dimensional model tests are carried out varying the length of ground anchors. The corresponding numerical simulations with finite element method using FEMtij-2D software are also carried out for the same scale of the model tests. Subloading t_{ij} model is used in the analyses to model the ground material. Displacement of the retaining wall, surface settlement of the ground, tensile force of the anchors, and the ground movement are investigated. It has been revealed that installation a longer anchor at the deeper excavation part is the most effective method in the ground anchors of earth retaining wall. The numerical analyses capture well the results of the model tests.

1 INTRODUCTION

Retaining wall is commonly used to prevent the ground deformation during open excavation. In addition, struts are used to make a large underground area in open excavation. However, sometimes the struts hinder the construction process as the excavated area is occupied with the struts. It is possible to excavate large section and to increase excavation depth using ground anchor as reinforcement in a retaining wall without strut, which accomplishes smooth handling of construction works. In present practical design method of retaining wall with anchor, earth pressure acting on the retaining wall and its stability as a whole are evaluated within rigid plasticity theory such as Rankine's earth pressure theory. The wall deflection is usually calculated using the beam spring model with Rankine's earth pressure theory, in the same way as that of the retaining wall with struts. In the literature (Yoo 2001), it is found that anchored wall has the restraining ability of wall movement greater than that of the braced wall, which emphasizes the necessity of investigating the mechanism of anchored wall. The purpose of this research is to investigate the mechanism of anchor type retaining wall by model tests and the corresponding numerical analyses. Analyses are performed using finite element method based on an elastoplastic constitutive model named subloading t_{ij} model (Nakai & Hinokio 2004).

2 LAYOUT OF MODEL TESTS

Figure 1 shows the schematic diagram of the two-dimensional apparatus. The size of the model ground is 680 mm in width and 450 mm in height. Aluminum rods of 5cm in length, having diameters of 1.6 mm and 3.0 mm and mixed with the ratio of 3:2 in weight, are used as the model ground (unit weight of the mass is 20.4 kN/m^3). The retaining wall is 300 mm in length, 60 mm in width and 0.5 mm in thickness, which is a plate of aluminum material (EI = 0.88 N*m^2/cm, EA = 4.22 kN/cm). It is set in the ground before excavation and is located at 200 mm from the right boundary of the ground. In the experiment the model ground was excavated with a layer of 15 mm in thickness up to a possible depth of excavation. The anchor plate is 50 mm in length, 50 mm in width and 5 mm in thick, and it is made of aluminum. In the anchor plate, aluminum rods of 1.6 mm diameter are glued at both sides at an interval of 10 mm to maintain a certain friction between the ground and the anchor plate. Pre-stress is applied at the head of the anchors. The pre-stress of the anchor is controlled by a fly nut

set up at its head, and the anchor can be set up at any arbitrary inclination (θ) from the horizontal line. The anchor is modeled connecting the head and the anchor plate by piano wire (thread) at both sides of the ground. The piano thread is 0.3 mm in diameter having $EA = 1.41*10^3$ kN/cm. Biaxial strain gages attached with a thin aluminum board (30 mm in length, 60 mm in width, and 0.2 mm in thickness) are connected in the piano thread to measure tensile force. By taking photographs with a digital camera and using PIV technique the ground movements and consequently the strain of the ground are measured. The wall deformation is also measured using digitizer from the photographs of the ground. A laser type displacement transducer is used to measure surface settlement of the ground.

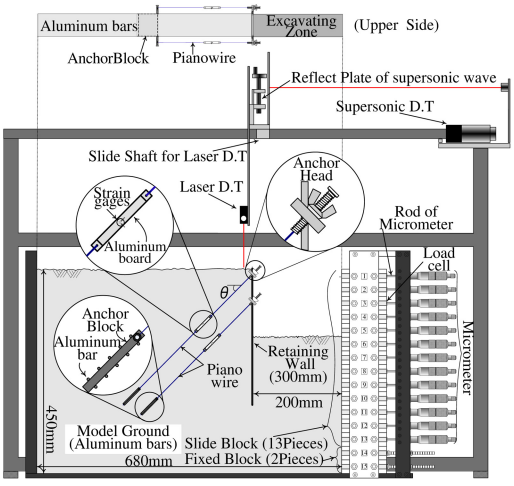

Figure 1. Apparatus of model tests.

Table 1. Pattern of model tests.

	Number of anchor	Initial tensile force (N)	Anchor length L (mm)	Angle θ°
Case 2-A	2	$T_1 = 0.31$	$L_1 = 150, L_2 = 125$	30
Case 2-B		$T_2 = 0.57$	$L_1 = 300, L_2 = 125$	
Case 2-C			$L_1 = 150, L_2 = 250$	
Case 2-D			$L_1 = 300, L_2 = 250$	

Table 1 shows the experimental pattern. The anchors are set up at 2 stages. Excavation depth during the installation of the 1st stage anchor is 30 mm and the 2nd stage anchor is 90 mm. The anchor depth for the 1st stage anchor is 15 mm and the 2nd stage anchor is 75 mm from the surface of the ground. A plane of active earth pressure is assumed considering the final excavation depth is 210 mm and angle of internal friction is 30°. The anchor plate is set up outside of the assumed plane of active earth pressure. Case 2-A is considered as the basic pattern, and experiments are carried out changing the length of the anchor. The initial pre-stress of the anchor is calculated from the active earth pressure using the prescribed excavation depth of each anchor as mentioned above. In this paper, only the results of the 2 stages anchor with the inclination of 30° will be presented due to the space limitation. These layouts of the model tests described above is determined referring to the previous research on the braced excavation with struts (Shahin et al., 2011) – i.e., the material of the ground, the size of the wall and the position of the supports and process of excavation are the same. In present model tests, the anchors are only used instead of the struts in the previous research.

3 LAYOUT OF NUMERICAL SIMULATIONS

An elastoplastic constitutive model for soils, called the subloading t_{ij}-model (Nakai & Hinokio 2004), is used in finite element analyses. This model requires only a few unified material parameters, but can describe properly the following typical characteristics of soils: (1) influence of intermediate principal stress on the deformation and strength of soil; (2) influence of stress path on the direction of plastic flow is considered by splitting the plastic strain increment into two components; (3) influence of density and/or confining pressure. Model parameters for the aluminium rod mass are shown in Table 2, which is the same as those used in the simulations of model tests using the aluminium rods mass for other geotechnical problems such as tunnelling, retaining wall problems (e.g., Shahin et al., 2011; Shahin et al., 2014; Nakai et al., 2007). The parameters are fundamentally the same as those of the Cam clay model except for the parameter a, which is responsible for the influence of density

Table 2. Material parameters for aluminum rod mass.

λ	0.008	Same parameters as Cam clay model
κ	0.004	
N(e_N at p = 98kPa)	0.30	
R_{CS}=$(\sigma_1/\sigma_3)_{CS\ (comp.)}$	1.8	
ν_e	0.2	
β	1.2	Shape of yield surface (same as original Cam clay if β = 1)
a	1300	Influence of density and confining pressure

and confining pressure. Where, λ and κ are the slope of loading and unloading curve of e-ln$p$ graphs at the normally consolidated line. N is the void ratio at mean principal stresses (p) 98 kPa in the normally consolidated line and ν_e is the Poisson's ratio. The parameter β controls the shape of yield surface. These parameters can easily be obtained from traditional laboratory tests. The parameters can be determined through conventional triaxial tests and consolidation test. Figure 2 shows the results of biaxial tests for the mass of aluminum rods used in the model tests. The figure shows the positive and negative dilatancy of aluminium rod mass; and it is clear that the strength and deformation behaviour are very similar to those of dense sand. The dotted lines are the calculated curves under $\sigma_1 = 0.2$ kPa, which almost corresponds to the stress level of the model tests.

Figure 3 shows a mesh used in the finite element analyses for the simulations of the model tests. The analyses are carried out using finite element code FEMtij-2D developed in Nagoya Institute of Technology. Isoparametric 4-noded elements are used to represent the soil. The mesh is well refined with elements of finer mesh in most regions. The sheet pile and anchor plates are modelled using elastic beam elements. The frictional behaviour (friction angle $\delta = 14°$) between the sheet pile and the ground is simulated using elastoplastic joint elements (Nakai 1985). The frictional angle, $\delta = 14°$, was obtained from a laboratory model test. The anchor is modelled using truss element as it can only resist tensile force. The stiffness of the truss element considered in the analyses is the same as the stiffness of the piano wire used in the model tests. In the analyses, the excavation is simulated removing elements in the mesh corresponding to the excavation area of the model tests. The analyses are carried out under plane strain conditions, since the aluminium rods do not deform in the out of plane direction. The analyses are carried out with the same conditions of the model tests. Both vertical sides of the mesh are free in the vertical direction, and the bottom face is kept fixed. The initial stresses of the ground are calculated by applying the body forces due to self-weight ($\gamma = 20.4$ kN/m^3), starting from a negligible confining pressure ($p_0 = 9.8 \times 10^{-6}$ kPa) and an initial void ratio $e = 0.35$. After self-weight consolidation the void ratio of the ground was 0.28 at the bottom and 0.30 at the top. The pre-stress is applied at the head of each anchor the same as the model tests.

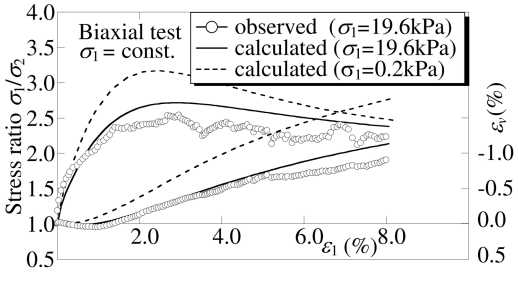

Figure 2. Stress-strain-dilatancy relation for aluminum rod mass.

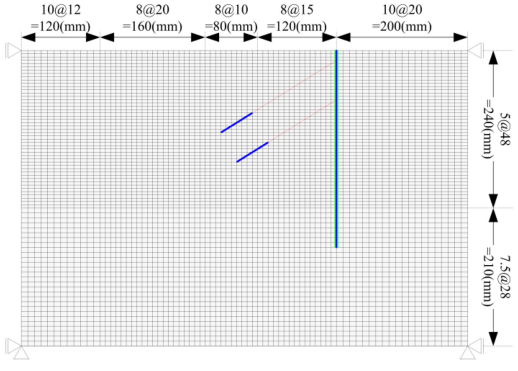

Figure 3. Mesh for finite element analyses.

4 SIMULATION OF PULLOUT BEHAVIOR OF ANCHOR BLOCK

The behavior of anchor block including its tensile strength has been investigated by a pullout test. Figure 4 shows the observed and computed results of the tests. The analyses are performed applying upward vertical displacement at the top most nodal point of the anchor block (beam element). Two tests are conducted varying the depth of the anchor from the surface of the ground (D), D = 15 and 30 cm. In the figure the marks represent experimental results and the lines show computed results. It is seen in the test results that pullout force of anchor block increases with the increasing vertical displacement and reaches an ultimate value following a reduction to some extent. The ultimate pullout load capacity of the deeper anchor block is larger than that of the shallower one. Although the numerical analysis shows the tendency of a flatter

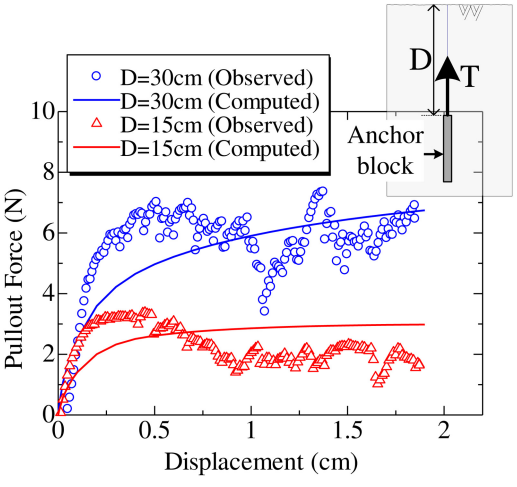

Figure 4. Tensile behavior of anchor block.

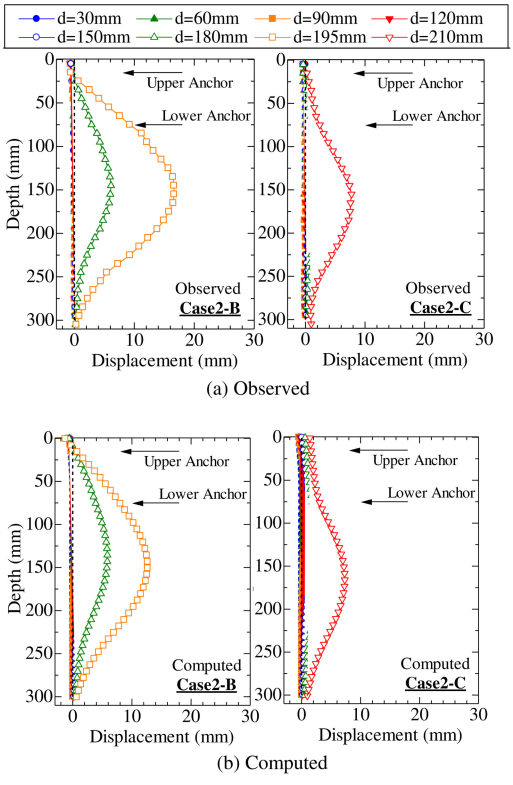

Figure 5. Horizontal displacement of wall in Case 2-B, C.

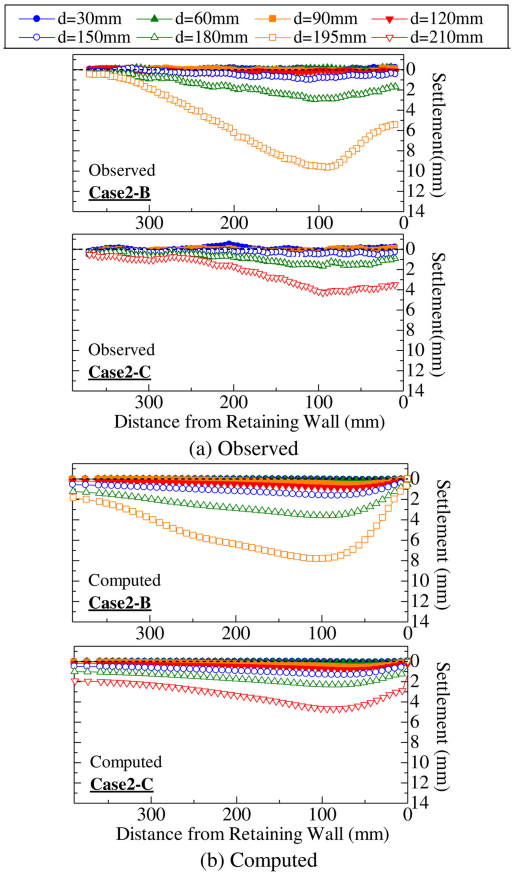

Figure 6. Surface settlement profiles in Case 2-B, C.

initial slope, it can mostly evaluate the ultimate pullout capacity and variation of the capacities with the soil depths the same way as the model tests. Therefore, the modeling of the anchor block in the numerical analysis can be considered as an appropriate one.

5 RESULTS AND DISCUSSIONS

5.1 *Settlement of ground and displacement of wall*

Figure 5 shows the observed (diagram (a)) and computed (diagram (b)) wall displacements for Case 2-B and Case 2-C where anchors are set at two stages in the ground. Figure 6 represents surface settlement profiles for the same set of tests. The legend represents excavation depth (d). The arrows in the figures indicate the position of the upper and lower anchors. It is revealed that for the two-stage anchors it restricts the wall displacement and surface settlement till the excavation depth of 150 mm irrespective of the anchor length. When excavation depth exceeds 150 mm a large wall displacement is observed near 150 mm depth of the wall, and the surface subsidence increases significantly as well. For the excavation depth of 180 mm, the influence of anchor length is seen remarkably. In Case 2-C (only the lower anchor length is longer) the wall displacement is smaller than that of Case 2-B (only the upper anchor length is longer). It (Case 2-C) also restricts the surface subsidence both in magnitude and in area, *i.e.* subsidence occur in narrower area. Therefore, if the lower anchor is longer, it is possible to make deeper excavation. The results of the numerical analyses show the same tendency of the model tests not only in shape but also in quantity for both wall displacement and surface settlement profiles as a whole.

Figure 7 represents the maximum horizontal displacement of the wall for the excavation depth of 150 mm and deeper where the wall displacement remarkably occurs. The figure shows the comparison of the results among Case 2-A, Case 2-B, Case 2-C and Case 2-D. As mentioned above, Case 2-C (only the length of the lower anchor is longer) restricts the wall displacement almost the same extent as Case 2-D where the lengths of both upper and lower anchors are longer. That is, the longer lower anchor produces supporting effect efficiently. On the other hand, only the longer upper anchor, Case 2-B, produces almost the same effect as Case 2-A where the lengths of both upper and lower anchors are shorter. In both Case 2-A and Case 2-B, displacement increases significantly when excavation depth crosses 180 mm and the ground collapses at shallower excavation depth compare to other two cases. The numerical simulation slightly

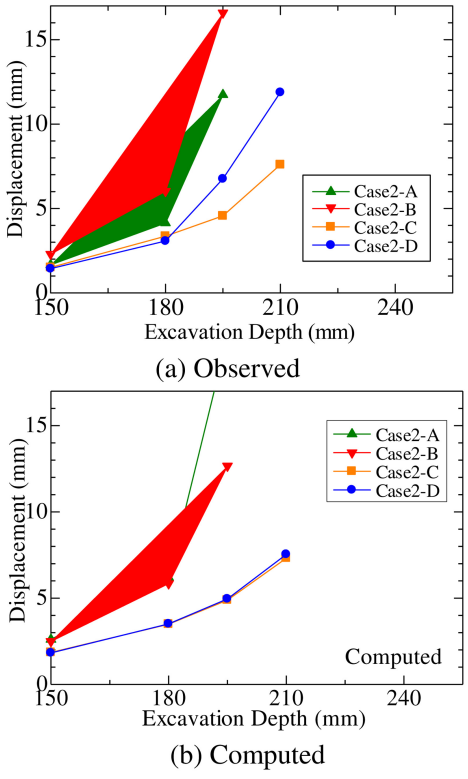

Figure 7. Wall horizontal displacement for excavation depth deeper than 150 mm.

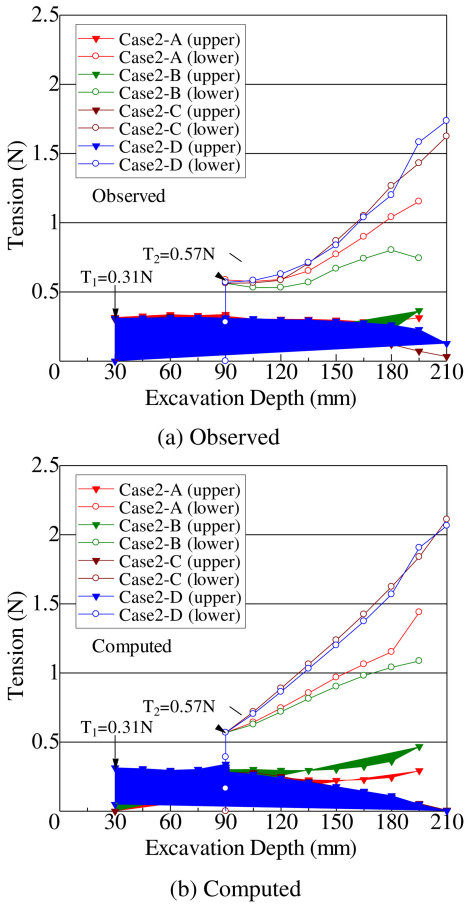

Figure 8. Variation of tensile force of anchor.

over-predicts the wall displacement of Case 2-A at excavation depth of 180 mm as some elements in the ground undergo into failure state. Until the collapses of the ground the analyses show good agreement with the model tests.

5.2 *Anchor tensile force*

Figure 8 shows the observed and computed variations of tensile force at both upper and lower anchors for Case 2-A to D. It is seen that for all cases, the change of tensile force at the upper anchor is less significant compare to the lower anchor. In contrast, the tensile force at the lower anchor increases with the advance of excavation, especially, when the excavation depth is deeper than 150 mm which is associated with a significant wall deformation and surface settlement of the backfill ground. In the case of longer lower anchor (Case 2-C, D), the maximum tensile force is almost 1.5times the maximum tensile force of the lower anchor of Case 2-A. The numerical analyses capture the observed tensile force of both upper and lower anchors.

5.3 *Distribution of shear strain in ground*

Figure 9 illustrates distribution of shear strain of the model tests and numerical simulations. The distributions of shear strain of the model tests are obtained using Particle Image Velocimetry (PIV) technique. In this paper, two images are divided into a finite area; the average movement rate of the mass of aluminum rods of each area is extracted as nodal displacements. The strain for one grid is calculated from these displacements by using the shape functions and the B matrix (strain-displacement matrix) that is usually used in finite element method to relate displacements and strains. It is seen that in Case 2-A, for the shorter anchor shear band develops outside the lump of the ground having the anchor block inside the lump. In the case of longer upper and lower anchors (Case 2-D), the anchor blocks are located far outside the slip surface which restricts the development of shear strain significantly. Case 2-C, where only the lower anchor is longer, shows almost the same distribution of shear strain as that of Case 2-D. This is because, as the lower anchor is located outside the slip surface and produces sufficiently high pullout resistance it increases tensile force and hence a notable supporting effect can be speculated. On the other, though the upper anchor block of Case 2-B is located outside the slip surface, there is not much difference of the distributions of shear strain between Case 2-A and Case 2-B. Therefore, it can be

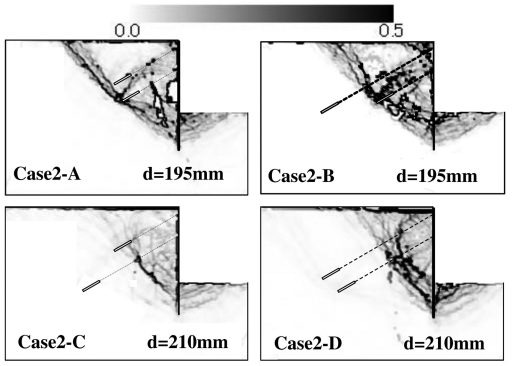

(a) Observed

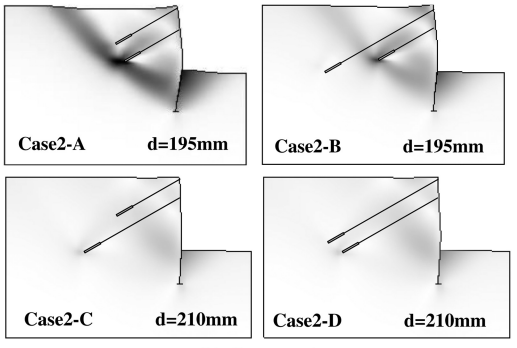

(b) Computed

Figure 9. Distribution of shear strain: Case 2-A to D.

said that a longer anchor at the lower excavation part restricts the displacement of retaining wall and can be treated as an effective supporting method. The shear strain of the numerical analyses shows good agreement with the results of the model tests.

6 CONCLUSIONS

Two-dimensional model tests and the corresponding numerical analyses were carryout out on anchor type braced excavation. It is revealed that supporting effect of anchor in braced excavation can be achieved if the anchor block is setup outside the assumed slip surface developed during excavation. Especially, longer anchor in the lower part of the excavation produces a significant supporting effect resisting wall displacement and surface settlement of the backfill ground. As the wall deformation and surface settlement of the backfill ground increase with the advance of excavation it is important to install an anchor with a sufficient length in deeper excavation depth. In contrast, there is not much difference in supporting effect between a shorter and a longer anchor in shallower excavation depth. Therefore, it is important to find out an optimum supporting pattern in anchor type braced excavation for rational design in the case economical point of view. It can also be concluded that the computed results in which typical stress-strain behavior of soils is appropriately taken into account agree well with the experimental results qualitatively and quantitatively. While the ground behavior of retaining wall with different length of the anchor in the present paper are explained in this paper, we will discuss the influence of the position and inclination of the anchors, the depth and stiffness of the wall and others in another paper in future.

The ground material used in the present model tests is the same as that of the previous model tests on other geotechnical problems such as the braced exaction with struts (e.g., Nakai et al. 2007; Shahin et al. 2011) and tunneling (e.g., Shahin et al. 2011; Shahin et al. 2014). The numerical simulations of these geotechnical problems including the present one were carried out using the same constitutive model (subloading t_{ij} model), and the unified material parameters was employed (see Table 1).

Since the constitutive model (subloading t_{ij} model) used in the present simulations is capable of soil behaviors from under low confining pressure in the model tests to under the stress level in real ground using unified material parameters, the present analytical method is applicable to the practical real problems as well.

ACKNOWLEDGEMENTS

This study is supported financially in part by the Grant-in Aid for Scientific Research (B-25289144, Teruo Nakai) from Ministry of Education, Science and Culture in Japan.

REFERENCES

Nakai, T. 1985. Finite element computations for active and passive earth pressure problems of retaining wall. *Soils and Foundations*, 25(3): 98–112.

Nakai, T. & Hinokio, T. 2004. A simple elastoplastic model for normally and over consolidated soils with unified material parameters. *Soils and Foundations*, 44(2): 53–70.

Nakai, T., Farias, M.M., Bastos, D. & Sato, Y. 2007. Simulation of conventional and inverted braced excavation using subloading t_{ij} model. *Soils and Foundations*, 47(3): 597–612.

Shahin, H.M., Kikumoto, M. & Uetani, Y. 2011. Influence of existing foundations on retaining wall in braced excavation. *Proc. of 14th Asian Reg. Conf. on Soil Mech. and Geotechnical Engineering*, *Hong Kong, May*, 267, CD-ROM.

Shahin, H.M., Nakai, T., Zhang, F., Kikumoto, M. & Nakahara, E. 2011. Behavior of ground and response of existing foundation due to tunneling, *Soils and Foundation*. 51(3): 395–409.

Shahin, H.M., Nakai, T. & Kuroi, S. 2014. Effect pf repeated shear deformation on single and tuin tunneling – model test and finite element analysis. Proc. of IS-Seoul 2014, (submitted).

Yoo, C.S. 2001. Behavior of braced and anchored walls in soils overlying rock. *Journal of Geotechnical and Geoenvironmental Engineering*, 127(3):225–233.